
B.A. NAJAFOV,¹ V.V. DADASHOVA²

¹Institute of Radiation Problems, Azerbaijan National Academy of Sciences
(9, B. Vakhbazade Str., Baku AZ1143, Azerbaijan Republic; e-mail: bnajafov@rambler.ru,
bnajafov@physics.ab.az, rovshan63@rambler.ru)

²Baku State University
(23, Academician Z. Khalilov Str., Baku, AZ1143, Azerbaijan Republic)

**OPTOELECTRONIC PROPERTIES OF THIN
HYDROGENATED $a\text{-Si}_{1-x}\text{Ge}_x\text{:H}$ ($x = 0\div 1$) FILMS
PRODUCED BY PLASMA CHEMICAL
DEPOSITION TECHNIQUE**

PACS 78.66.-w, 81.15.Cd

Possibilities of plasma chemical deposition of $a\text{-Si}_{1-x}\text{Ge}_x\text{:H}$ ($x = 0\div 1$) films undoped and doped with PH_3 or B_2H_6 have been analyzed from the viewpoint of their application in $p\text{-i-n}$ structures of solar cells. The optical, electric, and photo-electric properties are considered, and the amount of hydrogen contained in those films is determined. The film properties are found to strongly depend on the film composition and the hydrogenation level. The number of hydrogen atoms in the films is varied by changing the gas mixture composition, and IR absorption in $a\text{-Si:H}$ and $a\text{-Ge:H}$ films is measured. The photoconductivity is calculated using the formula $J_{\text{ph}} = AF^\gamma$ with $\gamma = 1$. The hydrogen concentration N_{H} in the films is characterized by the preferable additional parameter P and was determined with the use of the vibrational stretching and wagging modes for the $a\text{-Si}_{1-x}\text{Ge}_x\text{:H}$ ($x = 0\div 1$) films. The $a\text{-Si:H}$ and $a\text{-Si}_{0.88}\text{Ge}_{0.12}\text{:H}$ films were used to fabricate three-layer solar cells with an element area of 1.3 cm^2 and an efficiency of 9.5%.

Keywords: thin hydrogenated films, plasma chemical deposition, photoconductivity.

1. Introduction

Si films and their alloy are characterized by various structural phases. The most interesting of them are crystalline grains embedded in an amorphous matrix. Such alloys are prepared using various methods and under various technological regimes. For the films of hydrogenated amorphous silicon, $a\text{-Si:H}$, grown by the method of cyclic deposition with an annealing in hydrogen plasma, the Staebler–Wronski effect is weakly pronounced [1]. The authors of work [2] mark the actual absence of this effect in nanostructured $a\text{-Si:H}$ films. The crystallization of silicon $a\text{-Si:H}$ films is carried out by various methods, such as a long-term annealing in vacuum at $600\text{ }^\circ\text{C}$, a rapid thermal

treatment [3], laser annealing [4], and ionic implantation [5]. The mobility of charge carriers and the efficiency of doping in such films are higher than in $a\text{-Si:H}$, and the coefficient of optical absorption is higher than in crystalline silicon. The $a\text{-Si}_{1-x}\text{Ge}_x\text{:H}$ and $a\text{-Si}_{1-x}\text{C}_x\text{:H}$ films are an efficient cheap material for the manufacture of solar cells and other electronic devices [6, 7]. In this connection, the production of the films concerned and the modification of their conductivity type is a challenging problem.

In work [8], it was shown that a variation of the substrate temperature is accompanied by an increase of the nanocrystal growth rate. It was found that an increase of the PH_3 concentration gives rise to a reduction of both the average grain size d and the volume fraction V_c of crystalline particles. At the doping with boron and an increase of the B_2H_6 concentra-

tion, the value of d does not change, whereas V_c decreases. Hydrogen in a -Ge:H has weaker passivation properties than in a -Si:H, so that, in whole, the photoefficiency of a -Si_{1-x}Ge_x:H films is some lower than that of a -Si:H ones [10, 11].

Hydrogen atoms play an important role in the film structure. This work aims at determining the amount of hydrogen in the a -Si_{1-x}Ge_x:H ($x = 0 \div 1$) films and measuring their electrophysical properties, as well as at developing electronic devices on their basis.

2. Experimental Part

Thin a -Si_{1-x}Ge_x:H ($x = 0 \div 1$) films were fabricated using the method of plasma chemical deposition. The applied gas mixtures H₂ + SiH₄ and He + GeH₄ were taken in various proportions. The corresponding procedure was described in works [12, 13] in detail. Plasma was generated by an HF field owing to a mainly inductive coupling. The thickness of obtained films varied from 0.1 to 1.0 μm. For every specimen, the absorption, α , refraction, n , reflection, R , and transmission, T , coefficients, as well as the energy gap width E , were measured using the Tauc model [14]. Optical absorption was studied on an IKS-21 spectrometer, at room temperature, and following the procedure described in works [15, 16].

The measurement of the temperature dependence of the electric conductivity, $\sigma(T)$, in the interval 500 K ≤ T ≤ 200 K showed that, for a -Si_{1-x}Ge_x:H films, the $\sigma(T)$ behavior is governed by the band conductivity and is described by the known relation [17, 18]. At rather low temperatures, $T \leq 200$ K, the activation energy is a varying quantity obeying the Mott law. The photoconductivity calculated in the framework of the method of work [19] was found to satisfy the formula

$$I_{\text{ph}} = AF^\gamma \quad (1)$$

with $\gamma = 1$, where F is the flux of incident photons per surface unit (cm⁻² · s⁻¹). Integrated over the whole spectral range, the photon flux equaled 5×10^{12} cm⁻² · s⁻¹. Note that, in this wavelength interval, $N_0 \approx F$, where N_0 is the total number of incident photons irrespective of their wavelengths.

It is clear that, in order to determine the coefficient of proportionality A , the spectral regions of weak absorption should be used. The photocurrent was measured in the interval 0.5 ÷ 3.0 eV. For a -Si_{1-x}Ge_x:H

films, it was found that the variation of such parameters as the hydrogen concentration H , hydrogen content x , quantum yield η , and drift mobility μ gave rise to the photocurrent changes in the interval $10^{-8} \div 10^{-4}$ cm²/V.

3. Results and Their Discussion

The hydrogen concentration in the a -Si_{1-x}Ge_x:H ($x = 0 \div 1$) films was determined with the help of the method proposed by Brodsky *et al.* [15, 16]:

$$N = \frac{AN_A}{(\Gamma/\xi)} \int \frac{\alpha(\omega)}{\omega} d\omega, \quad (2)$$

where N_A is the Avogadro number, and $\Gamma/\xi = 3.5$ cm²/mol is the integral strength of hydride. If $\Delta\omega/\omega_0 \leq 0.1$, where ω_0 is the maximum of the absorption band and $\Delta\omega$ its width, Eq. (2) can approximately, to an error of ±2%, be rewritten in the form

$$N = \frac{AN_A}{(\Gamma/\xi)\omega_0} \int \alpha(\omega) d\omega, \quad (3)$$

where $A = \frac{(1+2\varepsilon)^2\varepsilon^{1/2}}{9\varepsilon^2}$, and ε is the dielectric constant ($\varepsilon = 12$ for Si and 16 for Ge). Designating the pre-integral expression in Eq. (3) as A_S and introducing the integrated absorption of the stretching mode for every film, $J_S = \int_{\omega_S} \alpha(\omega) d\omega$, we obtain the general short expression for the hydrogen concentration

$$N_H = A_S J_S. \quad (4)$$

The coefficient A_S equals 1.4×10^{20} cm⁻² for a -Si:H films in the stretching mode interval. The absorption coefficient α equals $8 \times 10^{-1} \div 3 \times 10^2$ cm⁻¹ at indicated frequencies (about 2100 cm⁻¹), and $N_H = 7 \times 10^{21} \div 2.1 \times 10^{22}$ cm⁻³ in this case. For a -Ge:H films, $A_S = 1.7 \times 10^{20}$ cm⁻². It is evident that Eq. (4) also characterizes the vibrational mode of bond stretching in the a -Si:H, a -Ge:H, and a -Si_{1-x}Ge_x:H films. Estimations of the relative hydrogen binding in hydrogenated amorphous a -Si_{1-x}Ge_x:H bring about the expression

$$P = \left\{ \frac{N_{\text{Si-H}}}{N_{\text{Ge-H}}} \right\} \frac{x}{1-x}, \quad (5)$$

where $N_{\text{Si-H}}$ and $N_{\text{Ge-H}}$ are the hydrogen concentrations in a -Si:H and a -Ge:H films, respectively. Equation (4) can be rewritten for the wagging

Characteristic parameters of amorphous $a\text{-Si}_{0.60}\text{Ge}_{0.40}\text{:H}$ films

No. Film	P_{H_2} , mTorr	E_0 , eV	P at.%	H, cm^{-3}	$N_{\text{Si:H}}$, cm^{-3}	$N_{\text{Ge:H}}$, cm^{-3}	N_{H} , cm^{-3}	$I_S^{(\text{Si})}$	$I_S^{(\text{Ge})}$	$J_W^{(\text{Ge})}, J_W^{(\text{Si})}$	I_S/I_W
1	0.6	1.32	1.85	1.3	6.2×10^{21}	2.2×10^{21}	3.1×10^{20}	7.2×10^1	6.3×10^1	6.0×10^2	0.13
2	1.2	1.36	2.29	5.1	9.4×10^{21}	2.7×10^{21}	4.0×10^{21}	8.6×10^1	7.5×10^1	5.2×10^2	0.18
3	1.8	1.41	2.59	8.7	1.3×10^{22}	3.3×10^{21}	5.1×10^{21}	9.4×10^1	8.3×10^1	4.0×10^2	0.26
4	2.4	1.44	3.38	14.7	2.1×10^{22}	4.1×10^{21}	6.2×10^{21}	1.0×10^2	9.0×10^1	3.0×10^2	0.38
5	3.0	1.52	4.16	23.7	2.9×10^{22}	4.6×10^{21}	9.7×10^{21}	1.1×10^2	1.0×10^2	2.7×10^2	0.51

mode of $a\text{-Si:H}$ and $a\text{-Ge:H}$ films. The corresponding quantities $N_{\text{Si-H}}$ and $N_{\text{Ge-H}}$ look like as follows:

$$N_{\text{H}} = A_W J_W. \tag{6}$$

Here, $J_W = \int_{\omega_w} \frac{\alpha(\omega)}{\omega} d\omega$ is the integral absorption of the wagging mode for the $a\text{-Si:H}$ and $a\text{-Ge:H}$ films, and $A_W = 1.6 \times 10^{19} \text{ cm}^{-2}$ and $1.1 \times 10^{19} \text{ cm}^{-2}$, respectively. Knowing the $N_{\text{Ge-H}}$ -value (where, for $a\text{-Ge:H}$ films, $A_W = 1.6 \times 10^{19} \text{ cm}^{-2}$ and $\alpha = 50 \text{ cm}^{-1}$), let us calculate the hydrogen concentration N_{H} in the $a\text{-Si}_{1-x}\text{Ge}_x\text{:H}$ film using the expression

$$N_{\text{H}} = N_{\text{Ge-H}}^{\text{wag}} \left\{ \frac{\int_{\text{streets}} \left(\frac{\alpha_1(\omega)}{\omega} \right) d\omega}{\int_{\text{streets}} \left(\frac{\alpha_2(\omega)}{\omega} \right) d\omega} \right\}, \tag{7}$$

where $N_{\text{Ge-H}}^{\text{wag}}$ is the number of Ge-H bonds calculated with the help of Eq. (6) for the wagging modes in pure $a\text{-Ge:H}$. The second multiplier in the expression for N_{H} (the integral ratio between the maxima of IR absorption) corresponds to the vibrational mode of stretching in the specimen and in pure $a\text{-Ge:H}$. For its calculation, the maximum corresponding to the vibrational stretching mode of Ge-H (2000 cm^{-1}) in the $a\text{-Si}_{1-x}\text{Ge}_x\text{:H}$ film was used.

The data presented above make it possible to estimate the oscillator strength in the $a\text{-Si}_{1-x}\text{Ge}_x\text{:H}$ film using the relation

$$\Gamma = J_S/J_W,$$

where $J_S \approx J_S^{\text{Ge}} + J_S^{\text{Si}}$ and $J_W \approx J_W^{\text{Ge}} + J_W^{\text{Si}}$. The quantities J_S^{Ge} , J_S^{Si} , J_W^{Ge} , and J_W^{Si} are the integral absorptions of the stretching and wagging modes, respectively. For the oscillator strength, we obtain $\Gamma = 0.51$ (at $x = 0$) and 0.13 (at $x = 1$). The maximum value of the parameter P ($P = 4.16$) is obtained for

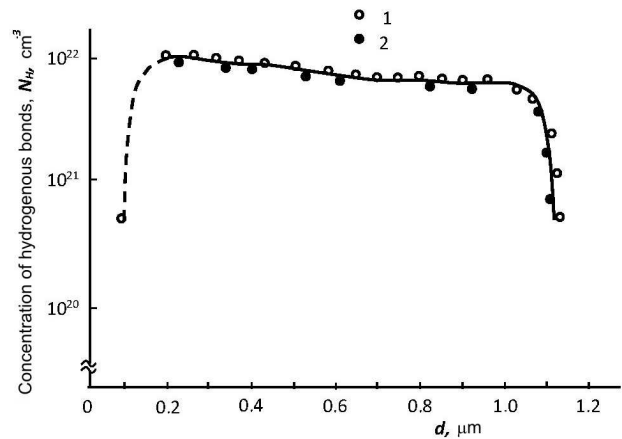


Fig. 1. Hydrogen distributions across the film thickness d determined by the proton recoil (1) and IR absorption spectrum (2) methods

$x = 0.40$. In Table, the characteristic parameters of amorphous $a\text{-Si}_{0.60}\text{Ge}_{0.40}\text{:H}$ films are presented.

Figure 1 demonstrates the hydrogen distribution across the film thickness d determined with the use of the recoil proton method (points 1) and the IR absorption spectrum (points 2). One can see that hydrogen atoms are distributed rather uniformly. Note that the values of N_{H} determined by the indicated techniques coincide to an accuracy of 2-3 at. %.

In Fig. 2, the correlation dependences of the hydrogen concentration determined for the $a\text{-Si}_{0.60}\text{Ge}_{0.40}\text{:H}$ films with the help of the effusion method are depicted. One can see that the hydrogen concentration N_{H} determined in this way correlates with the corresponding values calculated, by using the integrated strength J_W at a wagging mode frequency of 600 cm^{-1} . After the effusion at the thermal treatment ($350 \div 700 \text{ }^\circ\text{C}$), the hydrogen concentration was found to equal $C_{\text{H}} = 1.3 \div 23.7 \text{ at. \%}$.

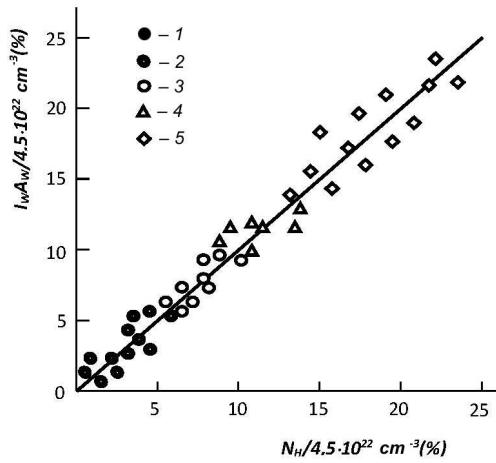


Fig. 2. Correlation dependences of the hydrogen concentration determined by the effusion method for $a\text{-Si}_{0.60}\text{Ge}_{0.40}\text{:H}$ films obtained at various hydrogen pressures $P_{\text{H}_2} = 0.6$ (solid circles), 1.2 (bold circles), 1.8 (thin circles), 2.4 (triangles), and 3.0 mTorr (diamonds)

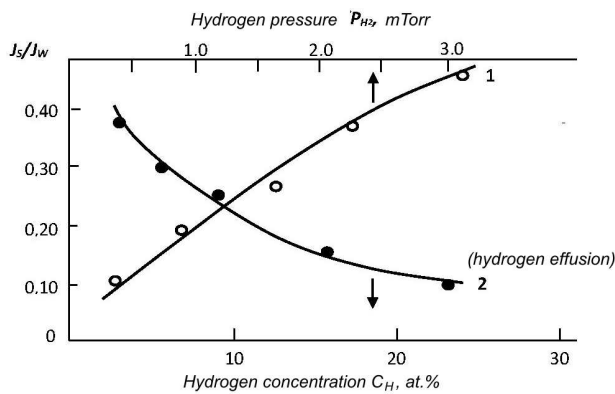


Fig. 3. Dependences of the partial hydrogen pressure P_{H_2} (1) and the hydrogen concentration C_{H} (2) on the oscillator strength Γ in amorphous films of the solid solution $a\text{-Si}_{0.60}\text{Ge}_{0.40}\text{:H}$

It is also found that the oscillator strengths Γ depend on the hydrogen concentration C_{H} : they decrease at the hydrogen effusion. As the hydrogen content P_{H_2} in the environment of the obtained $a\text{-Si}_{0.60}\text{Ge}_{0.40}\text{:H}$ films increased (within the partial pressure interval from 0.6 to 3.0 mTorr), the oscillator strength grew (Fig. 3). This circumstance is related to the increase of the numbers of hydrogen-containing bonds GeH and SiH at the specified frequency. As the annealing temperature grows, the Ge-H and Si-H bonds break. The hydrogen concentration in the $a\text{-Si:H}$ films after the thermal treatment at 350 °C

starts to decrease, and at 700 °C it practically vanishes [20]. The shift of the absorption band in the solid with respect to the characteristic frequency of this vibration mode in a gas can be determined, by using the expression [21]

$$\Delta\omega = - \left[\frac{e^{*2}}{2mR^3\omega_0} \right] \left[\frac{\varepsilon - 1}{2\varepsilon + 1} \right], \quad (8)$$

where e^* is the effective charge, m the reduced dipole mass, R the radius of a sphere around the volume including the dipole, and ε the dielectric permittivity of the matrix. The quantity e^* can be determined from the relation

$$Z = \frac{cn\omega}{2\pi^2} \frac{m}{e^{*2}}, \quad (9)$$

where c is the light velocity, n the refractive index, and ω the oscillation frequency. The obtained theoretical values coincide with the experimental data.

3.1. Optical properties of films

The dependence of the quantity $(\alpha h\nu)^{1/2}$ on $h\nu$ enables one to determine the energy gap width for every film [14,16]. In all examined films, the optical absorption edge coefficient is described by the relation

$$\alpha h\nu = B (h\nu - E_0)^2, \quad (10)$$

where $\alpha = 5 \times 10^4 \div 10^5 \text{ cm}^{-1}$, E_0 is the corresponding optical energy gap width for a specific film, and B is the proportionality factor. The specific value of the latter is determined by extrapolating the dependence of $(\alpha h\nu)^{1/2}$ on $h\nu$ for every specimen. The square-law dependence (10) was obtained theoretically in the framework of the Tauc model [14] describing the density of states in the mobility gap. The B -values obtained for $a\text{-Si}_{1-x}\text{Ge}_x\text{:H}$ ($x = 0 \div 1$) films varied from 527 to 343 $\text{cm}^{1/2}/\text{eV}$, and the corresponding E_0 -values from 1.14 to 1.86 eV.

3.2. EPR spectra of amorphous $a\text{-Si}_{1-x}\text{Ge}_x\text{:H}$ films

The EPR spectra of $a\text{-Si}_{1-x}\text{Ge}_x\text{:H}$ films were registered on an RE-1316 spectrometer with an operation frequency of 9.4 GHz ($B = 3.2 \text{ cm}$) at a temperature of 80 K. The resulting spectra were asymmetric, because they consisted of two components associated with free Si and Ge bonds. However, the observed

signal was not a simple superposition of signals for Si and Ge: those signals strongly interacted with each other, so that the ultimate signal registered in the intermediate interval tended to look like as a single one. Therefore, the observed spectra to the left and to the right can be described by a superposition of those two components: with the factor $g = 2.018 \div 2.022$ and a linewidth of 73–86 Gs for silicon free bonds, and with the factor $g = 2.004 \div 2.006$ and a linewidth of 51–65 Gs for germanium ones [10].

For $a\text{-Si}_{1-x}\text{Ge}_x\text{:H}$ films, the $g(x)$ values are smaller in comparison with the values of 2.005 for free silicon bonds and 2.018 for free germanium ones. In other words, in Si–Ge systems, the value of g for free silicon or germanium bonds diminishes [10]. In Fig. 4, the typical EPR curves for $a\text{-Si}_{1-x}\text{Ge}_x\text{:H}$ films with $x = 0.20$ are shown. The g -factor was determined by doubly integrating the differential curves. The results were reduced to a common scale with the use of a MgO:Mn^{2+} standard.

3.3. Electric and photo-electric properties of $a\text{-Si}_{1-x}\text{Ge}_x\text{:H}$ films

The results of dark conductivity measurements for the films concerned testify that this parameter can be presented as a sum of two components: high- (at $T \geq 200$ K) and low-temperature (at $T \leq 200$ K) ones:

$$\sigma = \sigma_1 + \sigma_2 = \sigma_{01} \exp\left(-\frac{\Delta E}{kT}\right) + \sigma_{02} \exp\left(-\frac{\Delta E}{kT}\right). \quad (11)$$

For $a\text{-Si}_{1-x}\text{Ge}_x\text{:H}$ films with x varying within the interval $0 < x < 1$, the quantity ΔE changes from 0.5 to 1.0 eV. Depending on x , the localization radius in $a\text{-Si}_{1-x}\text{Ge}_x\text{:H}$ films at temperatures $500 \text{ K} \geq T \geq 200 \text{ K}$ amounts to $\alpha^{-1} = 7 \div 10 \text{ \AA}$, the density of states to $N(E_F) = 10^{16} \div 10^{18} \text{ cm}^{-3} \text{ eV}^{-1}$, the jump energy to $E = 0.012 \div 0.091 \text{ eV}$, and the hopping distance to $R = 70 \div 150 \text{ \AA}$.

In Fig. 5, the dependences of the energy gap width on the conductivity activation energy are shown for $a\text{-Si}_{1-x}\text{Ge}_x\text{:H}$ films with $x = 1$ (1), 0.75 (2), 0.6 (3), 0.5 (4), 0.4 (5), 0.3 (6), 0.1 (7), and 0 (8). The pre-exponential coefficients in Eq. (11) change within the intervals $\sigma_{01} = 0.001 \div 50 \text{ } \Omega/\text{cm}$ and $\sigma_{02} = 10^{-7} \div 10^{-4} \text{ } \Omega/\text{cm}$. The introduction of 40 at.% Ge into $a\text{-Si:H}$ films resulted in a strong reduction of the

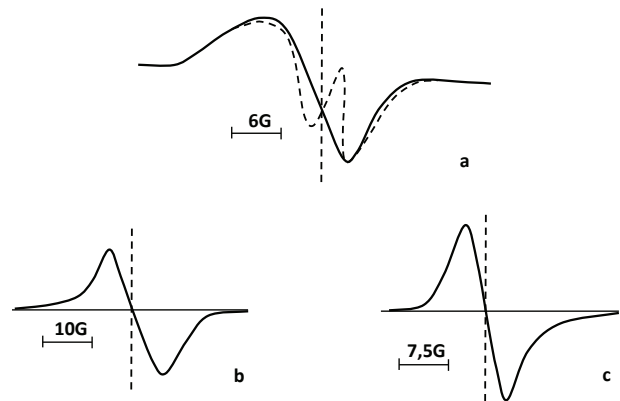


Fig. 4. Typical EPR curves registered at a temperature of 80 K: (a) $a\text{-Si}_{1-x}\text{Ge}_x\text{:H}$ with $x = 0.4$, $H = 21$ at.%, $g = 2.006$; (b) $a\text{-Si:H}$: $g = 2.005$ before the annealing and 2.003 after the annealing at $550 \text{ }^\circ\text{C}$; (c) $a\text{-Ge:H}$: $g = 2.018$ before the annealing and 2.003 after the annealing at $550 \text{ }^\circ\text{C}$

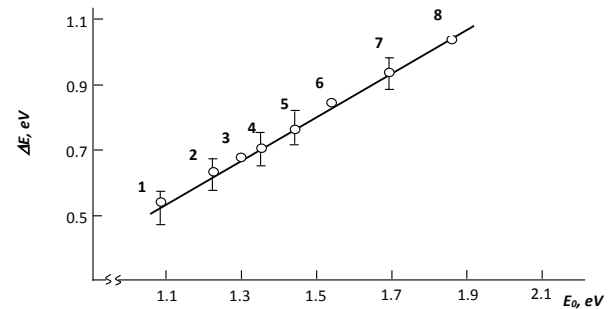


Fig. 5. Dependence of the energy gap width on the photoconductivity activation energy for $a\text{-Si}_{1-x}\text{Ge}_x\text{:H}$ films with $x = 1$ (1), 0.75 (2), 0.60 (3), 0.50 (4), 0.40 (5), 0.30 (6), 0.2 (7), and 0 (8)

electron and hole mobilities, energy gap width, photoconductivity, recombination lifetime, and conductivity activation energy (Fig. 7).

In the interval of a weak absorption, $A = 1$ and $\gamma = 0.4 \div 0.9$. The results obtained testify that the parameter γ depends only on the concentration of Ge atoms in $a\text{-Si:H}$ films (Fig. 6).

3.4. Creation of solar cells

The results of our researches showed that $a\text{-Si}_{1-x}\text{Ge}_x\text{:H}$ ($x \geq 0.20$) films can be used in semiconductor electronics as a high-quality material. For this purpose, we developed a three-layer element on the basis of two-layer elements of the cascade type. The three-layer element was fabricated from a two-layer

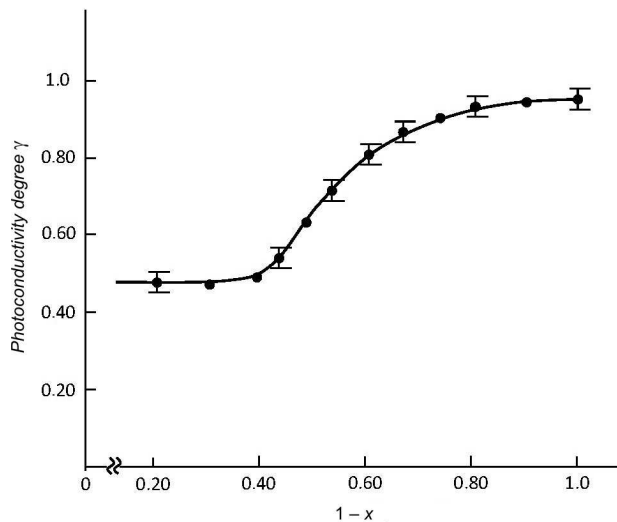


Fig. 6. Dependence of the photoconductivity parameter γ on the silicon concentration for $a\text{-Si}_{1-x}\text{Ge}_x\text{:H}$ films with $x = 1$ (1), 0.75 (2), 0.60 (3), 0.50 (4), 0.40 (5), 0.30 (6), 0.2 (7), and 0 (8)

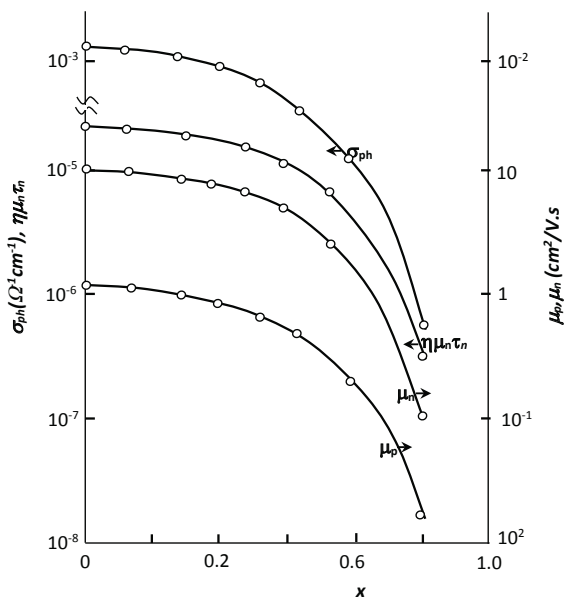


Fig. 7. Dependences of the photoconductivity parameters $\nu\mu_D\tau$ and σ_{ph} , and the drift mobilities for holes (μ_p) and electrons (μ_n) on the Ge concentration for $a\text{-Si}_{1-x}\text{Ge}_x\text{:H}$ films with $x = 0 \div 1$. Deposition conditions are indicated in Fig. 5

one consisting of two $a\text{-Si:H}$ -based elements with a $p\text{-i-n}$ junction, and a $p\text{-i-n}$ element, in which an $a\text{-Si}_{0.88}\text{Ge}_{0.12}\text{:H}$ film played the role of an i -layer (Fig. 8). The thicknesses of i -layers for the upper

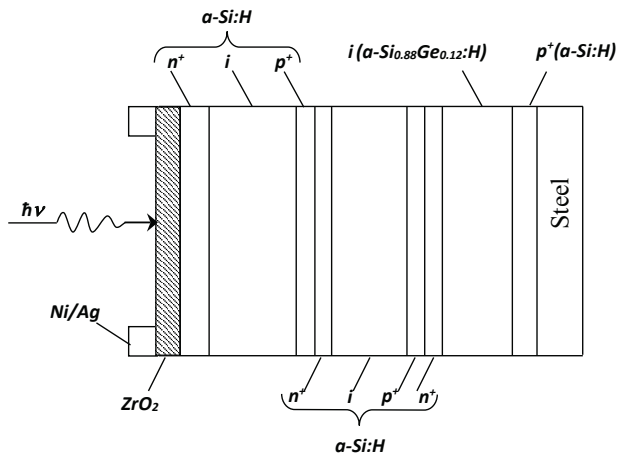


Fig. 8. Schematic diagram for the structure of a three-layer element with the i -layer fabricated on the basis of $a\text{-Si}_{0.88}\text{Ge}_{0.12}\text{:H}$

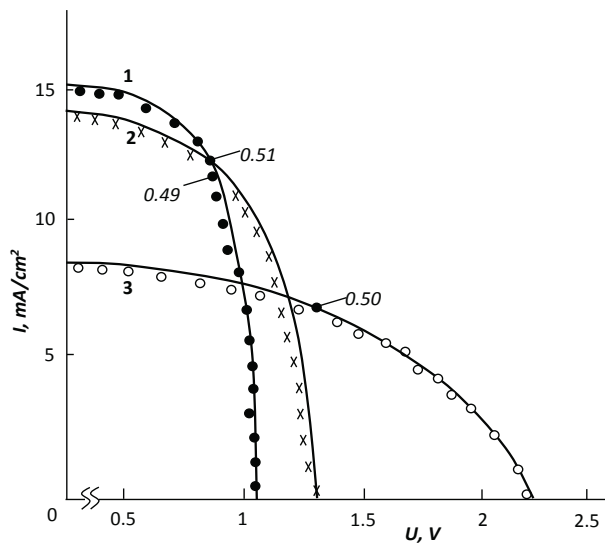


Fig. 9. Characteristics of solar cells with single-, two-, and three-layer $p\text{-i-n}$ structures at an illumination intensity of 100 mW/cm^2

junctions were selected to satisfy the equality condition for the short circuit current in the lower element: the short circuit current should amount to about half the corresponding value for the element with one $p\text{-i-n}$ junction. As the number of imposed layers grew, the open circuit voltage increased, and the short circuit current decreased. This method can be used to build up several layers (i.e. to fabricate an n -layer element). Note that an i -layer $0.5 \mu\text{m}$ in thickness was made for every element. The area of every element

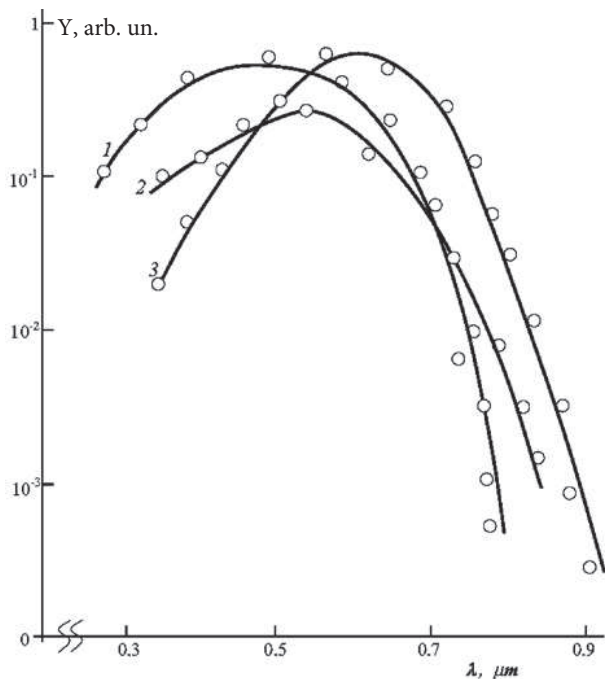


Fig. 10. Dependences of the charge carrier collection efficiency on the light wavelength for solar cells with single- (1), two- (2), and three-layer (3) $p-i-n$ structures

amounted to 1.3 cm^2 . While fabricating three-layer solar cells, all elements must have the same thickness and area. Steel was selected as a material for the substrate. As a coating material, ZrO_2 with a light transmittance of 80% was used. Simultaneously, ZrO_2 played the role of the upper (front) contact (Fig. 8). The thicknesses of $a\text{-Si:H}$ layers of the p - and n -types were equal to about 300 and 400 Å, respectively.

At doping the film, the amount of B_2H_6 and PH_3 in the gas mixtures was varied within the limits of 0.1 and 0.5%, respectively. After the deposition of amorphous semiconductor layers, ZrO_2 films about 500 Å in thickness were created by evaporation. Ni/Ag was used for the upper contacts, and the substrates made of a stainless steel for the lower ones. The elements were illuminated with a sunlight source under the AM-1 conditions (100 mW/cm^2). The short circuit current for three-layer elements was 8.5 mA/cm^2 , the open circuit voltage about 2.25 V, the filling coefficient about 0.50, and the efficiency η about 9.5% (Fig. 9). The efficiency was equal to 7% for the single-layer element and 8.9% for the two-layer

one. In Fig. 10, the dependences of the collection efficiency on the light wavelength at a photon flux of $10^{16} \div 10^{18} \text{ photon/m}^2/\text{s}$ are depicted for the single-, two-, and three-layer elements operating in the short circuit regime.

The efficiency of charge carrier collection at various wavelengths is defined as

$$Y(\lambda) = \frac{J_{\text{ph}}(\lambda)}{eN(\lambda)}, \quad (12)$$

where $J_{\text{ph}}(\lambda)$ is the photocurrent density, $N(\lambda)$ the number of photons incident on a surface unit per second, and e the charge of free carriers. In order to make the solar cell efficiency η higher, one has to increase the number of layers, decrease the area of elements, make a proper choice of metal wires, reduce the resistance of metal contacts, and so on.

4. Conclusions

The method of plasma chemical deposition with the use of the gas mixtures $\text{H}_2 + \text{SiH}_4$ and $\text{H}_2 + \text{GeH}_4$ taken in various proportions was applied to fabricate thin $a\text{-Si}_{1-x}\text{Ge}_x\text{:H}$ films with $x = 0 \div 1$. The absorption coefficient for visible light and the energy gap width were shown to increase as the silicon content in the films grew. The mobility of charge carriers and the photoconductivity in the $a\text{-Si}_{1-x}\text{Ge}_x\text{:H}$ films were found to strongly decrease if the germanium concentration exceeds 40 at.%. Solar cells on the basis of $a\text{-Si:H}$ and $a\text{-Si}_{0.88}\text{Ge}_{0.12}\text{:H}$ films were fabricated: single-, two-, and three-layer structures were created, and their parameters were measured. In particular, the corresponding efficiency η was determined to equal 7, 8.9, and 9.5%, respectively, provided the same element area of 1.3 cm^2 . For the three-layer element, the maxima of the collection efficiency were shifted toward the long-wave region. No degradation was observed in the obtained structures at their illumination with light in the wavelength interval from 0.3 to 1.1 μm for 120 h. The structures on the basis of $a\text{-Si}_{0.88}\text{Ge}_{0.12}\text{:H}$ and $a\text{-Si:H}$ films were demonstrated to be effective in the fabrication of solar cells, so that the further works aimed at improving the film quality and increasing their efficiency are challenging.

1. V.P. Afanas'ev, A.S. Gudovskikh, and V.N. Nevedomskii *et al.*, *Fiz. Tekh. Poluprovodn.* **36**, 238 (2002).
2. O.A. Golikova, M.M. Kazanin, and V.Kh. Kudoyarova, *Fiz. Tekh. Poluprovodn.* **32**, 484 (1998).

3. M.M. Mezdragina, A.V. Abramov, G.M. Masina *et al.*, Fiz. Tekh. Poluprovodn. **32**, 620 (1998).
4. O.A. Golikova and U.S. Babakhodzhaev, Fiz. Tekh. Poluprovodn. **36**, 1259 (2002).
5. O.A. Golikova, A.N. Kuznetsov, V.Kh. Kudoyarova, and M.M. Kazanin, Fiz. Tekh. Poluprovodn. **31**, 816 (1997).
6. *The Physics of Hydrogenated Amorphous Silicon*, edited by J.D. Joannopoulos and G. Lukovsky (Springer, Berlin, 1984).
7. B.A. Najafov, in *Proceedings of the Intern. Conference on Amorphous and Microcrystalline Semiconductors* (Polytechnical Inst. Publ. House, Saint-Petersburg, 2006), p. 51.
8. H. Colder, R. Rizk, M. Morales, P. Marie, J. Vicens, and J. Vickridge, J. Appl. Phys. **98**, 024313 (2005).
9. R.R. King, D.C. Zaw, K.M. Edmontson, C.M. Fetzer, G.S. Kinzey, H. Yoon, R.A. Sherif, and N.H. Kazam, Appl. Phys. Lett. **90**, 231 (2007).
10. *Amorphous Semiconductors. Technologies and Devices*, edited by Y. Hamakawa (North-Holland, Amsterdam, 1983).
11. B.A. Najafov, G.I. Isakov, and V.R. Figarov, Prikl. Fiz., No 4, 107 (2004).
12. B.A. Najafov, Int. Sci. J. Altern. Ener. Ecol. Solar Energy No. 11, 177 (2007).
13. B.A. Najafov and G.I. Isakov, Int. Sci. J. Altern. Ener. Ecol. Solar Energy, No 4(24), 79 (2005).
14. J. Tayes, R. Grigorovici *et al.*, J. Non-Cryst. Solids **15**, 627 (1966).
15. M.N. Brodsky, M. Cardona, and J.J. Cuomo, Phys. Rev. B **16**, 3556 (1977).
16. B.A. Najafov and G.I. Isakov, Zh. Prikl. Spektrosk. **72**, 371 (2005).
17. N.F. Mott and E.A. Davies, *Electronic Processes in Non-Crystalline Materials* (Oxford Univ. Press, Oxford, UK, 1979).
18. B.A. Najafov, Fiz. Tekh. Poluprovodn. **34**, 1383 (2000).
19. R.A. Rudder, J.W. Cook, and G. Fucovsky, Appl. Phys. Lett. **45**, 887 (1984).
20. B.A. Najafov and V.R. Figarov, Int. J. Hydrog. Energy **35**, 4361 (2010).
21. B.A. Najafov and G.I. Isakov, Int. Sci. J. Altern. Ener. Ecol. Solar Energy No. 4(24), 74 (2005).

Received 23.11.12.

Translated from Ukrainian by O.I. Voitenko

B.A. Наджафов, В.В. Дадашова

ОПТОЕЛЕКТРОННІ ВЛАСТИВОСТІ
В ГІДРОГЕНІЗОВАНИХ ТОНКИХ ПЛІВКАХ
 $a\text{-Si}_{1-x}\text{Ge}_x\text{:H}$ ($x = 0-1$), ОТРИМАНИХ
ПЛАЗМОХІМІЧНИМ ОСАДЖЕННЯМ

Резюме

Проаналізовано можливості застосування технології плазмохімічного осадження плівок $a\text{-Si}_{1-x}\text{Ge}_x\text{:H}$ ($x = 0-1$), нелегованих і легованих PH_3 і V_2H_6 , для використання їх в $p-i-n$ -структурах сонячних елементів. Розглянуто оптичні, електричні, фотоелектричні властивості, також визначено кількість водню, що міститься в даній плівці. Знайдено, що властивості плівки сильно залежать від складу і рівня гідрогенізації. Кількість атомів водню в плівках варіювали шляхом зміни складів газової суміші, і вимірювали ІК поглинання для плівок $a\text{-Si:H}$ і $a\text{-Ge:H}$. Фотопровідність розраховано за співвідношенням: $J_{\text{ф}} = AF^{\gamma}$ при $\gamma = 1$. Концентрацію водню в плівках визначено переважним додатковим параметром – P . Водночас N_{H} визначено за допомогою коливальної моди розтягування і моди кочення для плівок $a\text{-Si}_{1-x}\text{Ge}_x\text{:H}$ ($x = 0-1$). На основі плівок $a\text{-Si:H}$ і $a\text{-Si}_{0,88}\text{Ge}_{0,12}\text{:H}$ виготовлено тришарові сонячні елементи з площею елемента $1,3 \text{ см}^2$ і ефективністю (ξ) 9,5%.